2008

The Highly Similar *Arabidopsis* Homologs of Trithorax ATX1 and ATX2 Encode Proteins with Divergent Biochemical Functions

Abdelaty Saleh
University of Nebraska-Lincoln

Raul Alvarez-Venegas
University of Nebraska-Lincoln

Mehtap Yilmaz
University of Nebraska-Lincoln

Oahn-Le
University of Nebraska-Lincoln

Guichuan Hou
University of Nebraska - Lincoln

See next page for additional authors

The Plant Cell, Vol. 20: 568–579, March 2008, www.plantcell.org © 2008 American Society of Plant Biologists

The Highly Similar *Arabidopsis* Homologs of Trithorax ATX1 and ATX2 Encode Proteins with Divergent Biochemical Functions [W]

Abdelaty Saleh,[a,b] Raul Alvarez-Venegas,[a,c] Mehtap Yilmaz,[a,d] Oahn-Le,[a] Guichuan Hou,[a,e] Monther Sadder,[a,f] Ayed Al-Abdallat,[a,f] Yuannan Xia,[g] Guoqinq Lu,[h] Istvan Ladunga,[i] and Zoya Avramova[a,1]

[a] School of Biological Sciences, University of Nebraska, Lincoln, Nebraska 68588-0118
[b] North Carolina State University, Raleigh, North Carolina 27606
[c] Department of Genetic Engineering, Centro de Investigación y de Estudios Avanzados, Campus Guanajuato, Irapuato, C.P. 36821, Mexico
[d] Department of Cell and Molecular Biology, Boston University, Boston, Massachusetts 02215
[e] Microscopy Facility, Appalachian State University, Boone, North Carolina 28608
[f] Faculty of Agriculture, University of Jordan, Amman 11942, Jordan
[g] Genomics Core Research Facility, Center for Biotechnology, University of Nebraska, Lincoln Nebraska 68588-0665
[h] Department of Biology, University of Nebraska, Omaha, Nebraska 68182-0040
[i] Center for Biotechnology and Department of Statistics, University of Nebraska, Lincoln, Nebraska 68588-0665

Gene duplication followed by functional specialization is a potent force in the evolution of biological diversity. A comparative study of two highly conserved duplicated genes, *ARABIDOPSIS TRITHORAX-LIKE PROTEIN1* (*ATX1*) and *ATX2*, revealed features of both partial redundancy and of functional divergence. Although structurally similar, their regulatory sequences have diverged, resulting in distinct temporal and spatial patterns of expression of the *ATX1* and *ATX2* genes. We found that ATX2 methylates only a limited fraction of nucleosomes and that ATX1 and ATX2 influence the expression of largely nonoverlapping gene sets. Even when coregulating shared targets, ATX1 and ATX2 may employ different mechanisms. Most remarkable is the divergence of their biochemical activities: both proteins methylate K4 of histone H3, but while ATX1 trimethylates it, ATX2 dimethylates it. ATX2 and ATX1 provide an example of separated K4 di from K4 trimethyltransferase activity.

INTRODUCTION

Gene duplication, followed by functional divergence of the resulting pair of paralogous proteins, is a major force shaping molecular networks in living organisms (Ohno, 1970). Duplicated genes involved in signal transduction and transcription regulation might have been preferentially retained (Blanc and Wolfe, 2004). A duplicated transcription factor (TF) might lead to the origination of a nonoverlapping pathway to function in two different cell types, developmental stages, or environmental conditions. Because epigenetic regulators modulate expression of a large number of functionally linked genes (Alvarez-Venegas et al., 2007a), a duplicated gene encoding an epigenetic factor might contribute to the evolution of novel gene networks.

The highly conserved SET peptide [for Su(var)3-9, E(z), Trithorax], encoded by the *Drosophila melanogaster Su(var)39-*, *E(z)-*, and *Trithorax*-related genes, carries histone lysine methyltransferase (HKMT) activity with a preference for specific histone residue substrates (Rea et al., 2000). Although *SET* domain genes are ancient (Alvarez-Venegas et al., 2007b), they have proliferated in eukaryotes, particularly after the transition to multicellularity (Alvarez-Venegas and Avramova, 2002; Krauss et al., 2006). The genes from the *Trithorax* family encode factors that can modulate chromatin structure through their abilities to methylate the N-terminal lysine 4 of histone H3 (H3K4). *Trithorax* homologs have been found in both animals and plants, suggesting that common mechanisms of epigenetic regulation are derived from a shared ancestor. Subsequently, each lineage has evolved distinct subgroups of duplicated genes to meet lineage-specific needs.

According to current models, duplicated genes (paralogs) may have remained with redundant functions or may have acquired different fates: one copy might have been silenced to become nonfunctional or the two versions might have parceled out the range of pleiotropic functions of the ancestral gene. The latter path may lead to separation of functions or subfunctionalization (Kondrashov et al., 2002). A general limitation of theoretical models is that it is unclear how closely biology follows. While it is logical to expect that structurally divergent paralogs might have evolved novel functions, it is impossible to predict the functions of duplicated genes with highly conserved coding sequences.

The *Arabidopsis thaliana TRITHORAX* family, *ATX*, contains five homologs segregating into two well-supported sister clades (Baumbusch et al., 2001; Alvarez-Venegas and Avramova, 2002). ATX1 and ATX2, originating from a segmental chromosomal duplication, belong in the same clade as sister paralogs.

[1] Address correspondence to zavramova2@unl.edu.
The author responsible for distribution of materials integral to the findings presented in this article in accordance with the policy described in the Instructions for Authors (www.plantcell.org) is: Zoya Avramova (zavramova2@unl.edu).
[W] Online version contains Web-only data.
www.plantcell.org/cgi/doi/10.1105/tpc.107.056614

Interesting questions regarding the fate of the ATX2 and ATX1 paralogs are whether they have retained redundant functions, whether one copy has lost its function, or whether the two have acquired divergent functions. The only member of the ATX family for which a biochemical function has been established is ATX1, which is involved in trimethylating histone H3-lysine 4 (H3K4me3) (Alvarez-Venegas et al., 2003). However, ATX1 is not responsible for the genome-wide methylation of histone H3K4: ~85% of the H3K4me3 signal is still present in the *atx1* mutants, suggesting that other methyltransferases are involved as well (Alvarez-Venegas and Avramova, 2005).

The degree of H3K4 methylation (mono-, di-, or trimethylated K-NH_2-groups) has important consequences for the transcriptional activity of pertinent genes in yeast and animal chromatins (Bernstein et al., 2002; Milne et al., 2002; Nakamura et al., 2002; Santos-Rosa et al., 2002; Ng et al., 2003; van Dijk et al., 2005; Kouzarides, 2007). In *Arabidopsis*, dimethylated K4 (H3K4me2) was found at coding regions independent of whether the gene was active or not but was absent from intergenic regions, suggesting that H3K4me2 could be a general mark distinguishing potentially transcribed from nontranscribed sequences in the genome (Alvarez-Venegas and Avramova, 2005).

In yeast and animal systems, the same enzyme establishes both H3K4me2 and H3K4me3 marks: SET1 in *Saccharomyces cerevisiae* and the human trithorax homologs MLL1, MLL2, and hSet1 can produce mono-, di-, and trimethyl H3K4 marks (Bernstein et al., 2002; Santos-Rosa et al., 2002; Wysocka et al., 2005; Ruthenberg et al., 2007). However, the mammalian germ cell–specific factor Meisetz carries out K4 tri- but not mono- or dimethylation (Hayashi et al., 2005). Known histone H3K4 trimethyltransferases from *Arabidopsis* do not display dimethylating activity (Alvarez-Venegas and Avramova, 2005; Kim et al., 2005). Despite the broad distribution of the H3K4me2 in euchromatin (Jasencakova et al., 2003; Lippman et al., 2004) and its association with transcribed sequences (Alvarez-Venegas and Avramova, 2005), enzyme activity generating H3K4me2 marks in *Arabidopsis* has not been identified. Here, we report that the *ATX2* encodes a putative H3K4 dimethyltransferase, providing an example of separated histone K4 dimethyltransferase and K4 trimethyltransferase activities in *Arabidopsis*.

Experimental design and data interpretation were performed in the context of a hypothesis that after duplication, the functions of ATX1 and ATX2 have diverged. Their possible functional divergence was assessed by (1) testing the ability of ATX1 and ATX2 to substitute for each other, as an indication of redundancy; (2) establishing patterns of expression of *ATX1/2* in the plant; (3) identifying genes regulated by each ATX as an illustration of their specificity/redundancy, and (4) analysis of their biochemical functions.

RESULTS

Structural Relationship and Origin of the *ATX1* and *ATX2* Genes

The SET and the PHD (plant homeotic domain) domains are signature features of TRITHORAX family proteins of both animal and plant origin. In addition, two conserved peptides (FYR-C and FYR-N), together called DAST (for Domain Associated with SET in Trithorax; Alvarez-Venegas and Avramova, 2001), are located adjacent to each other in a subset of trithorax proteins. The presence or absence of DAST correlates with the division of *Arabidopsis* trithorax proteins in two subgroups (Baumbusch et al., 2001; Alvarez-Venegas and Avramova, 2002).

The *ATX1* and *ATX2* paralogs have originated from a segmental chromosomal duplication (Baumbusch et al., 2001; Figure 1A). The regions immediately surrounding *ATX2* and *ATX1* on chromosomes 1 and 2, respectively, are in reverse orientation, with collinearly positioned conserved paralogous genes interspersed with genes of no apparent similarity. All genes conserved between the two chromosomal regions have preserved their orientations with respect to the ATX gene, suggesting that the nonconserved genes are the products of insertions or deletions that have taken place since the duplication.

ATX1 and ATX2 are 65% identical and 75% similar at the amino acid level. The two proteins have similar architectural motifs (Figure 1B). To determine whether structural similarity translates into functional redundancy, we analyzed two *atx2* lines (SALK_001880 and SALK_117262) with insertions in the promoter *(atx2-1*) and in the SET domain (*atx2-2*), respectively (Figure 2A). No transcripts could be amplified from the *ATX2* gene sequences in *atx2-1* plants, while *atx2-2* mutant plants produced a truncated message with a disrupted SET domain sequence (see Supplemental Figure 1A online). However, neither of the homozygous *atx2* mutant lines displayed obvious phenotypes. In contrast with the early bolting of *atx1* under both long- and short-day conditions, mutant *atx2* lines did not differ detectably from the wild type (Figure 2B). Upon maturation, *atx2* plants were indistinguishable from the wild type (Figure 2C). We could not detect flower defects similar to those in *atx1* (Alvarez-Venegas et al., 2003), except for the observation that ~20% of *atx2* flowers had delayed abscission of sepals and petals after fertilization (see Supplemental Figure 1B and Supplemental Table 1 online).

At a first glance, the lack of phenotypes and the inability of ATX2 to substitute for ATX1 in the *atx1* mutants appeared to support nonfunctionalization of *ATX2* following the duplication: extant *ATX1* continues to play the ancestral function, while *ATX2* has become nonessential. Further analyses, however, revealed more nuanced relationships between the *ATX1* and *ATX2* paralogs.

Differential Expression of *ATX1* and *ATX2* during Development

By being expressed in different temporal and/or spatial manners, redundant genes may acquire functional divergence (Pickett and Meeks-Wagner, 1995). To test this idea for the *ATX1*/*ATX2* pair, we generated transgenic lines expressing the β-glucuronidase (GUS) coding region behind the *ATX1* or *ATX2* promoters (see Methods for the respective promoter regions used). Potential involvement of regulatory sequences located in introns could not be assessed by this approach. Five and seven independently transformed lines, for *ATX1* and *ATX2*, respectively, each segregating for a single T-DNA insertion, were isolated and examined for GUS expression in various tissues in early development and later, at the flowering stage.

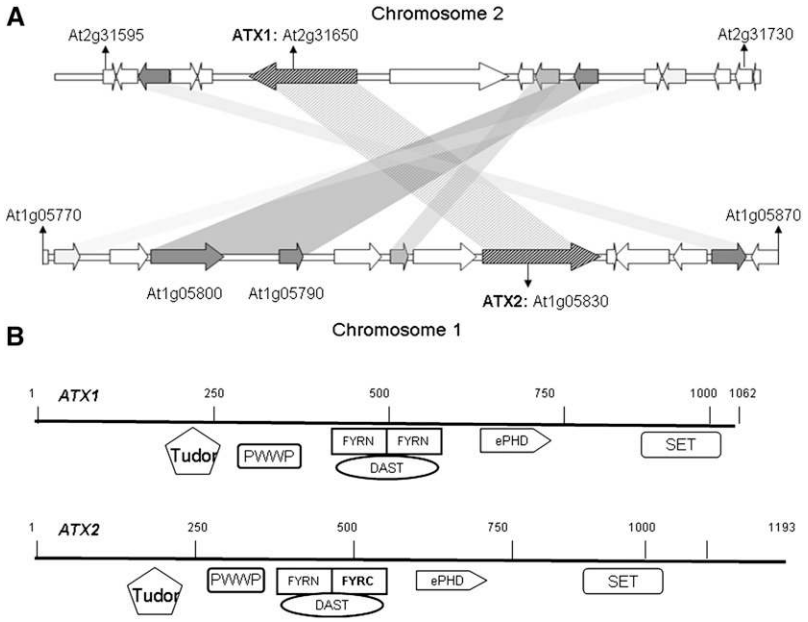

Figure 1. Structural Domains of ATX1 and ATX2 Proteins and Organization of the *ATX1* and *ATX2* Gene Loci.

(A) *ATX1*, *ATX2*, and flanking genes representing ~50-kb regions of chromosomes 2 and 1, respectively, drawn to scale. Arrows represent genes and the direction of their transcription; identities of the genes flanking the examined regions are shown on top. Orthologous genes are connected by shaded areas; empty arrows are noncolinear genes. The *At1g05800* and *At1g05790* genes are products of either tandem duplication in the ATX2 region or the deletion of one copy from chromosome 2.

(B) Schematic representation of the ATX1 and ATX2 protein motifs. The PHD domain belongs to a family called extended (ePHD); the closely positioned FYRN-FYRC domains form the DAST motif conserved in animal and plant Trithorax homologs; the PWWP and Tudor motifs are not found in metazoan Trithorax-related proteins. The SET domain is the most highly conserved peptide shared by the proteins of the SET1/Trithorax family found in all eukaryotic genomes.

Striking differences were observed at the early stages of development: the absence of GUS expression driven by the *ATX2* promoter in the tissues of young seedlings contrasted with the strong expression of GUS under the *ATX1* promoter (Figure 3A). Later in development, the *ATX2* promoter was activated as well, as illustrated by the blue staining of rosette leaves and roots (Figures 3B and 3C). The results suggested that *ATX1* is expressed throughout development, while expression of *ATX2* occurs later in life.

Apparently inactive in young roots, ProATX2:GUS expression was weakly stimulated in 2-week-old roots, although not in the vasculature (Figures 3A and 3B); *ATX2* promoter activity appeared much stronger at 5 weeks as blue staining was seen in all root tissues. The tips of the lateral roots were not stained, which was in contrast with roots of the same aged plants expressing ProATX1:GUS. The expression of *ATX1* in roots is under developmental in addition to tissue-specific regulation. In contrast with ProATX2, however, ProATX1:GUS is active in the vascular tissues of 6-d-old and 2-week-old roots. Later, the *ATX1* promoter is turned on in adjacent tissues as well, suggesting that in older roots, the *ATX1* and *ATX2* expression patterns may overlap. Apparently, only ATX1 is expressed in dividing root tip cells at this stage.

In aerial tissues, the *ATX1* promoter was active in rosette leaves, in growing inflorescence stems (in the upper younger regions), in cauline leaves (at hydathodes), and in the mature flowers (Figures 3C and 3D). P-*ATX2* was weakly active in inflorescence nodes and at the base of the flowers, where *ATX2*-GUS expression overlapped with *ATX1*-GUS expression.

In flowers, except for common (but weak) staining at the tips of the stigma, *ATX1* and *ATX2* displayed distinct domains of expression (Figure 3D). The *ATX1* promoter drives GUS expression in sepals, in the vasculature of petals, and in the filaments of the stamens. By contrast, *ATX2*-driven GUS expression was detected in pollen only. The tissue-specific staining within the same organ (stamens) illustrates spatial separation of *ATX1*/*ATX2* expression.

According to available data on TF binding sites (see Methods), both promoters carry putative sites for regulation by light, UV radiation, pathogen attack, wounding, and abscisic acid (see Supplemental Figure 2 online). However, more putative TF binding sites were recognized upstream of *ATX1* than of *ATX2*, suggesting that *ATX1* is subjected to a broader array of regulatory signals than is *ATX2.*

Genome-Wide Expression Analyses of *atx2* Mutant Plants

Collectively, the results so far imply that *ATX1* and *ATX2* encode both specific and redundant functions. Transcription profiling of genes with altered expression in *atx1* and *atx2* backgrounds offers a strategy to assess the functional divergence of the two paralogs at the genomic level.

Affymetrix gene chips (ATH1 Genome Arrays, with ~24,000 *Arabidopsis* genes) were used in whole-genome expression

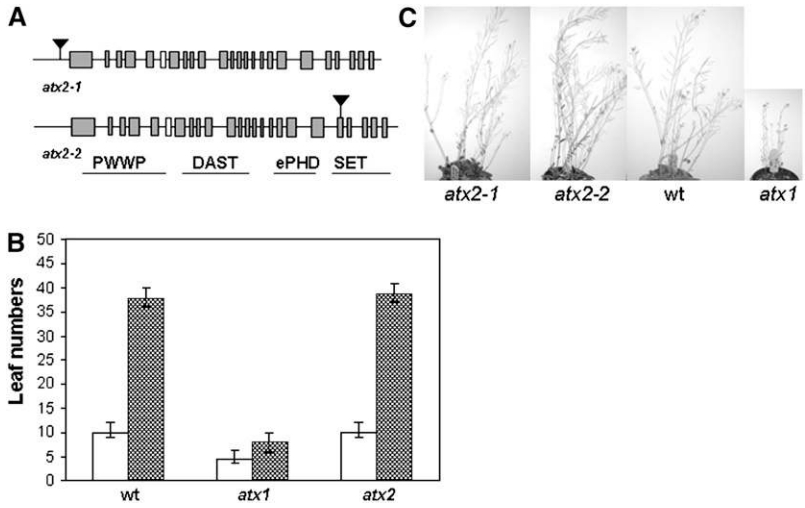

Figure 2. *atx2* Mutants and Phenotypes.

(A) Molecular structure of the *ATX2* gene, as established earlier (Alvarez-Venegas and Avramova, 2001) is drawn to scale. Shaded boxes indicate exons; empty boxes are true exons but are annotated as introns in the database. Triangles show *Ti*-insertions in the respective mutant lines. The lines below the genomic regions illustrate the position of the conserved domains encoded by *ATX2*.

(B) Wild-type, *atx1*, and *atx2-1* lines grown under long-day (18 h light/6 h dark) and short-day (9 h light/15 h dark) conditions shown as open and closed columns, respectively. The mean ± SE of rosette leaves at bolting (1-cm inflorescence stems) are shown for each sample ($n = 60$).

(C) Five-week-old plants grown in pots under 16-h-light/8-h-dark conditions. Pictures are taken at the same magnification.

analysis of *atx1* and *atx2* homozygous mutant plants. RNA was isolated from two independent biological replicates of *atx1*, *atx2-2*, and from control wild-type plants, grown and handled under the same conditions; each experimental sample was analyzed versus each of the two wild-type control sets (see Methods). Expression patterns reflected whole-plant gene expression and not tissue-specific profiles.

We consistently detected ~60% of all expressed *Arabidopsis* genes in all samples tested under the reported experimental conditions (Alvarez-Venegas et al., 2006a, 2006b) (correlation coefficients: 0.93 for *atx2*, 0.97 for *atx1*, and 0.98 for the wild type). Performing multiple test corrections by the highly conservative Bonferroni method restricting false discovery rate (Benjamini and Hochberg, 1995), we identified 80 genes with altered expression in the *atx2* background: 27 genes had increased, while 53 genes had decreased expression in *atx2* mutant plants compared with the wild type; ~900 genes changed expression levels in *atx1*mutant plants. Derepressed and repressed genes resulting from ATX2 loss of function are listed in Supplemental Data Sets 1 and 2 online. Data from the hybridization experiments in the *atx1* background are available elsewhere (Alvarez-Venegas et al., 2006a). Quantitative RT-PCR assays were consistent with the microarray data and confirmed the validity of the hybridization experiments (see below). Fewer genes altered transcription levels in *atx2* than in *atx1* backgrounds, suggesting a more limited role for ATX2 in *Arabidopsis.*

Shared ATX1/ATX2 Targets

Overlap analysis provides a general strategy for distinguishing unique from redundant functions. Analysis of *atx1*- and *atx2*-affected genes in the four possible combinations is shown by the Venn diagram (Figure 4). Among the 80 ATX2-regulated genes, 34 genes (~42%) overlapped with the ATX1-regulated set. Therefore, 58% of the ATX2 targets were not shared with ATX1 and were ATX2 specific. Within the shared set, only eight genes were coregulated (one upregulated and seven downregulated). Interestingly, 26 shared genes changed expression in opposite directions, implying that ATX1 and ATX2 might have opposite effects upon the expression of these genes. To further elucidate these relationships at the molecular level, we tested a possible contribution by ATX2 to genome-wide H3K4 methylation and explored the roles of ATX1 and ATX2 in H3K4 nucleosomal modification at three selected loci.

ATX2 and Genome-Wide Methylation of H3K4

Because ATX1 is not responsible for genome-wide methylation of H3K4 (Alvarez-Venegas and Avramova, 2005), we asked whether ATX2 contributes to the overall methylated profiles. Histones isolated from wild-type and from *atx2-2* mutant plants were analyzed by protein gel blot assays using antibodies specifically recognizing the H3K4 di- or trimethylated isoforms. The *atx2* line used in these analyses has a disrupted SET domain, allowing us to correlate H3K4 methylation patterns with the availability of the ATX2-SET peptide. To determine subtler variations in methylation levels, the amounts of loaded histone H3 in each sample were established with antibodies specific against nonmethylated H3; signal intensities of bands obtained with methylation-specific antibodies were normalized against the respective histone H3 amounts in 3-week-old mutant and wild-type plants.

In four independent measurements, the overall histone modification levels for either H3K4me2 or H3K4me3 varied between 2 and 6%, entirely within the standard error (see Supplemental

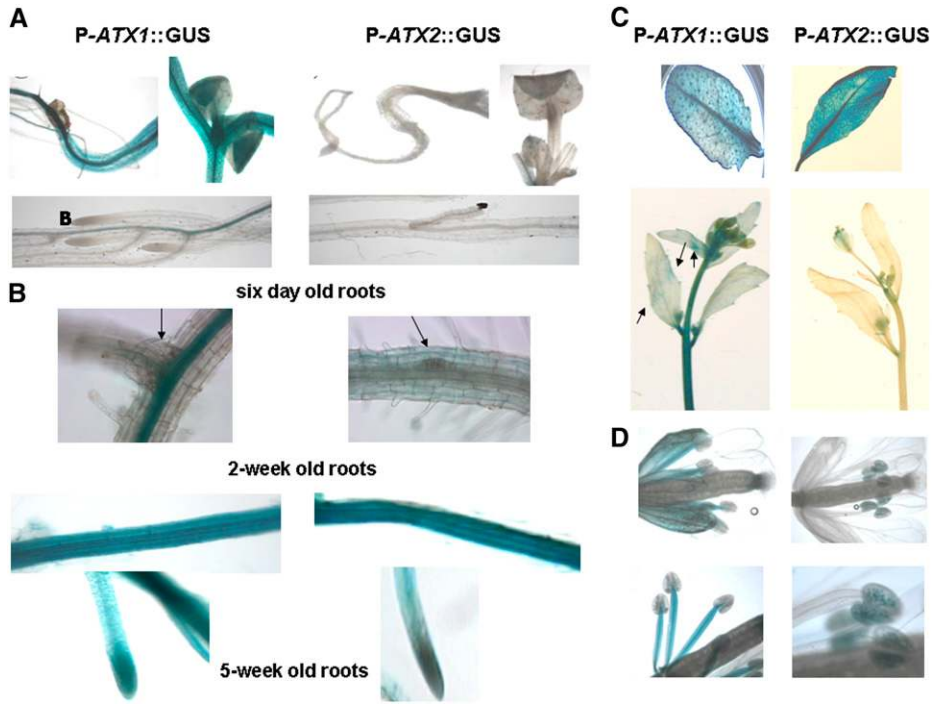

Figure 3. Expression of Pro*ATX1:GUS* and Pro*ATX2:GUS* during Development.

(A) GUS expression under the control of the *ATX1* or *ATX2* promoter (left side and right side, respectively) in transgenic plants is shown. Six-day-old seedlings are shown in all panels, except the top right panel, which shows a 2-week-old plantlet. The *ATX1* promoter is active in all tissues, particularly in the vasculature. In the roots, blue stain is seen only in differentiated vascular tissues. By contrast, the *ATX2* promoter is apparently inactive in young seedlings ($n = 16$, five lines) even in two-week-old plantlets.
(B) Later in development, P-ATX1 and P-ATX2 show both complementary and overlapping expression patterns in roots. Two- and five-week-old roots are shown in the top two and bottom four panels, respectively. Pro*ATX1:GUS* expression (left panels) in two-week-old roots is seen in vascular tissues but not in adjacent tissues or in emerging lateral roots (arrow). In 5-week-old roots, broader domains of Pro*ATX1* expression include nonvascular tissues and the tips of lateral roots. Pro*ATX2* (right panels) is weakly active in 2-week-old transgenic roots, mainly in nonvascular tissues, but not in the dividing cells of bulging lateral roots (arrow). At the flowering stage, expression of Pro*ATX2:*GUS in roots overlaps with Pro*ATX1:GUS*, except at the tips.
(C) Tissues harvested from 5-week-old flowering plants. Both *ATX1* and *ATX2* promoters are active in rosette leaves, particularly in the vascular tissues. Only the top (younger) parts of primary inflorescence stems and patches of cauline leaf cells (arrows) show staining in plants carrying the Pro*ATX1:GUS* transgene. Pro*ATX2:GUS* showed more restricted expression domains and weaker expression in inflorescence stems and tissues.
(D) Domains of Pro*ATX1:GUS* and Pro*ATX2:GUS* expression in flowers. In addition to petals and sepals, Pro*ATX1:GUS* is expressed in stamens, particularly in the filaments; the P-*ATX2*-driven GUS expression is concentrated mainly in the pollen grains.

Figure 3 online). We conclude that ATX2 is not involved in genome-wide histone H3K4 di- or trimethylation. However, this result could not resolve whether ATX2 does not possess an HKMT activity (consistent with a function lost after gene duplication), whether it modifies only a small fraction of *Arabidopsis* histones (consistent with the limited spatial and temporal patterns of expression of the *ATX2* gene) or whether it is fully redundant (biochemically) with ATX1. To distinguish between these alternatives, we examined the methylation profiles at three shared loci.

NAP Gene Regulation by ATX1 and ATX2

The downregulated expression of *At1g69490* in the *atx1* and *atx2* backgrounds (Figures 5A and 5B) suggested that in the wild type, this gene was activated by both ATX1 and ATX2. *At1g69490* encodes a plant-specific TF from the NAC family (NAP, for *NAC-LIKE ACTIVATED* by *AP3*/*PI*) (Sablowski and Meyerowitz, 1998). *At1g69490* showed reduced, but still significant, expression in both *atx1* and *atx2* mutant flowers, suggesting that ATX1 and ATX2 cooperate to maintain *NAP*'s wild-type expression levels. To reveal the molecular basis of this synergistic activity, as well as a possible role of ATX2 in the K4 methylation of *NAP* nucleosomes, we performed chromatin immunoprecipitation (ChIP) analyses with wild-type, *atx1*, and *atx2* flower chromatins using specific antidimethylated and antitrimethylated H3K4 antibodies.

NAP nucleosomes in wild-type flower chromatin carry both H3K4me2 and H3K4me3 marks (Figure 5C). In *atx1*, the H3K4me2 band was present, but the H3K4me3 signal had disappeared, consistent with ATX1 being the sole H3K4 trimethyltransferase acting at the NAP locus. On the other hand, the presence of the H3K4me2 signal indicated that ATX1 is not needed for dimethylating *NAP* nucleosomes. Surprisingly, the H3K4 methylation pattern reciprocally changed in the *atx2* flower chromatin (Figure 5C). Disappearance of H3K4me2, but

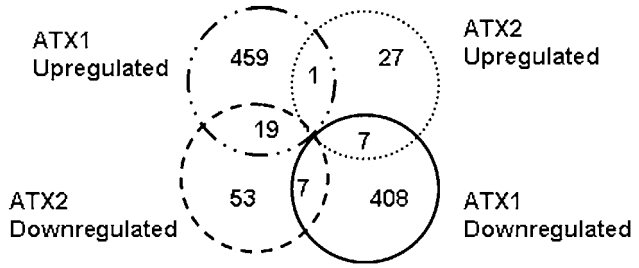

Figure 4. Venn Diagram of Genes with Altered Expression in *atx2-2* and *atx1*.

Overlapping genes with significantly altered expression from the microarray hybridization experiments examined in the four possible combinations. The genes in the *atx1* and *atx2* fractions represent the sets obtained after P values were subjected to multiple test corrections by the conservative Bonferroni method (see Methods). Overlaps indicate shared targets.

preservation of the H3K4me3 signal from *atx2-NAP*, nucleosomes implicated ATX2 in di- but not in tri-H3K4 methylation. The patterns of the housekeeping gene, *ACTIN7*, a control for the quality of the templates, was in full agreement with the reported data: the constitutively expressed housekeeping gene displayed both H3K4me2 and H3K4me3 bands (Figure 5D), confirming that missing signals from the *NAP* nucleosomes reflect specific ATX1 and ATX2 effects.

Thereby, *ATX2* encodes a putative H3K4 dimethyltransferase separate from the *ATX1*-trimethylating activity. The disappearance of the H3K4me2 signal in *atx2* correlates with lower expression from *NAP* despite the presence of H3K4me3. This observation is important because it suggests that both H3K4me2 and H3K4me3 marks are required for *NAP* expression at wild-type levels. The necessity to establish both marks on the *NAP* nucleosomes provides the basis for the synergistic interaction of *ATX1* and *ATX2* at the molecular level.

ATX1 and ATX2 Coregulate the *XTH33* Gene by Different Mechanisms

The *XTH33* gene (*At1g10550*), from the *Arabidopsis* xyloglucan endotransglucosylase/hydrolase (XTH) family, encodes a wall-modifying activity with a very tightly regulated expression in development (Becnel et al., 2006; Divol et al., 2007). Real-time PCR assays of several plant tissues confirmed that *XTH33* was expressed in flowers (see Supplemental Figure 4 online). Comparing *XTH33* expression in flowers of different backgrounds revealed a sharp decrease in transcript levels in *atx1* and *atx2* flowers (Figure 6A). H3K4me2 marks were present on wild-type and *atx1 XTH33* nucleosomes, although the signal appeared to be slightly reduced in the latter. However, H3K4me2 signal was undetectable on XTH33 nucleosomes in the *atx2* lines (Figure 6B), implicating ATX2 in this modification. Importantly, the loss of H3K4me2 marks from the *atx2 XTH33* nucleosomes,

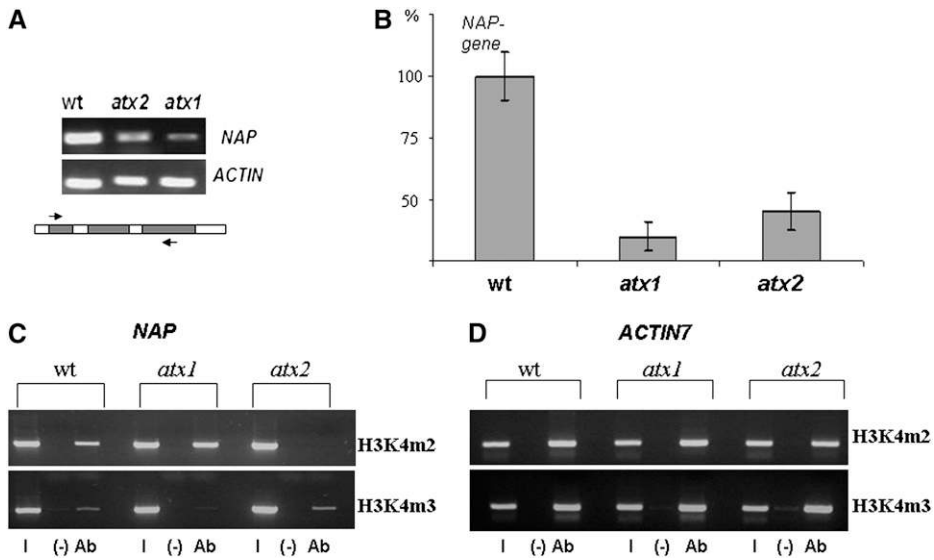

Figure 5. Expression and H3K4 Methylation Patterns of *NAP* in Wild-Type, *atx1*, and *atx2* Mutant Chromatin.

(A) *NAP* expression in wild-type, *atx2*, and *atx1* mutant flowers. The expression of *ACTIN7* is included as a loading control, and a schematic drawing of the *NAP* gene is shown below. Empty boxes represent introns, filled boxes are exons, and arrows indicate the locations of primers used for amplification in the RT-PCR **(A)** and ChIP assays **(C)**.

(B) Relative *NAP* transcript levels (mean ± SE) in wild-type, *atx2*, and *atx1* mutant flower chromatin as determined by real-time PCR ($n = 3$).

(C) *NAP* amplified from ChIP assays of wild-type, *atx1*, and *atx2* flower chromatin immunoprecipitated with antibodies distinguishing between di- and trimethylated H3K4 isoforms. I, input sample representing 10% of the template amount used for the immunoprecipitation. −, negative controls: samples treated in the same way as immunoprecipitated chromatins, except without added antibody.

(D) As in **(C)**, except that K4 methylation patterns of the housekeeping gene *ACTIN7* are shown as a control for the quality of the chromatins used as templates.

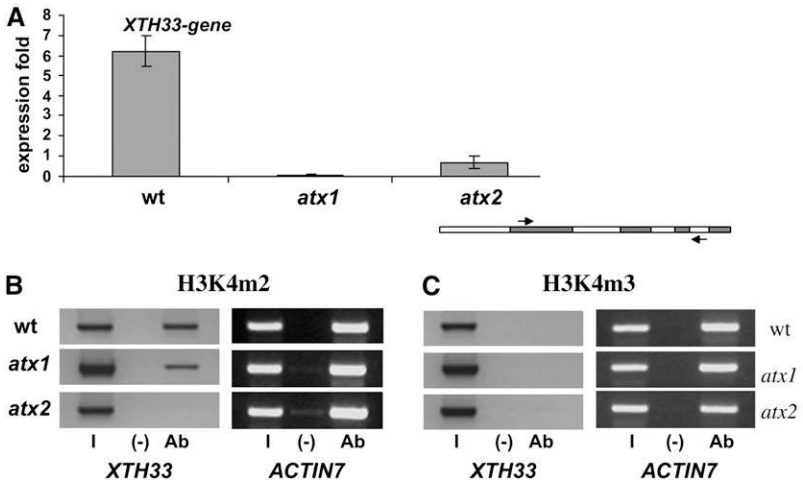

Figure 6. Expression and H3K4 Methylation Patterns of *XTH33* in Wild-Type, *atx1*, and *atx2* Chromatin.

(A) Fold differences in *XTH33* expression (mean ± SE, $n = 3$) in wild-type, *atx1*, and *atx2* mutant flowers as determined by real-time PCR.
(B) *XTH33* and *ACTIN7* amplified from ChIP assays of wild-type, *atx1*, and *atx2* flower chromatin immunoprecipitated with specific antibodies distinguishing dimethylated H3K4 (H3K4m2) isoforms. Labeling is as in Figure 5C. The methylation patterns of *ACTIN7* nucleosomes are shown as a control for the quality of the chromatins used as templates. A schematic illustration of the *XTH33* gene including the regions amplified for the ChIP assay is shown at the top of this panel.
(C) *XTH33* and *ACTIN7* amplified from ChIP assays of wild-type, *atx1*, and *atx2* flower chromatin immunoprecipitated with specific antibodies distinguishing trimethylated H3K4 (H3K4m3) isoforms. Labeling is as in Figure 5C.

accompanied by the decreased transcript levels, suggests that dimethylated H3K4 residues are required for *XTH33* expression. By contrast, H3K4me3 marks were absent from *XTH33* nucleosomes, including the transcriptionally active locus in the wild-type flower chromatin (Figure 6C). This feature, specific for the *XTH33* nucleosomes (confirmed by the presence of the *ACTIN7* bands amplified from the same DNA templates), reinforced the conclusion that H3K4me3 tags are not indispensable for active transcription of *Arabidopsis* genes (Alvarez-Venegas and Avramova, 2005). Accordingly, the decrease of *XTH33* transcripts in *atx1* flowers might reflect the inactivation of a TF driving *XTH33* expression in the absence of H3K4me3 and/or the subtle reduction in H3K4me2 marks. The different methylation patterns of *NAP* and *XTH33* nucleosomes illustrate that ATX1 and ATX2 use distinct mechanisms even when activating shared genes.

Differential Roles of ATX1 and ATX2 at the *WRKY70* Gene Locus

The *At3g56400* gene, encoding a TF from the WRKY family (WRKY70), is involved in the regulation of disease response genes at the intersection of two signaling pathways (Li et al., 2004, 2006). We have demonstrated that ATX1 directly associates with *WRKY70* nucleosomes, trimethylates H3K4 residues, and stimulates its transcription (Alvarez-Venegas et al., 2007a). Furthermore, we showed that H3K4me2 marks were present on all tested *WRKY70* nucleosomes regardless of whether *WRKY70* was actively transcribed (in wild-type leaves) or not (in wild-type flowers and in all tissues from the *atx1* mutants). Here, we examined whether ATX2 was involved in establishing the K4 dimethylation marks on *WRKY70*. First, we checked the transcriptional activity of *WRKY70* in the wild type and in *atx2-2* tissues by real-time PCR (Figure 7A). *WRKY70* is transcribed at basal levels in all tested tissues but is tissue-specifically activated in rosette leaves. In contrast with the sharp decrease in *WRKY70* transcripts in *atx1* leaves, *WRKY70* expression was not downregulated in the *atx2* background; it was even slightly augmented in the *atx2* stems (Figure 7A). The differential in the *WRKY70* transcript levels in *atx1* and in *atx2* rosette leaves (Figure 7B) illustrates the different effects upon *WRKY70* transcription exercised by ATX1 and ATX2. By ChIP assays, we show that both di- and trimethylated H3K4 marks were present on wild-type *WRKY70* leaf nucleosomes. The lower *WRKY70* transcript levels, accompanied by the disappearance of the H3K4me3 signal in *atx1* leaf chromatin (Figure 7C), were in full agreement with ATX1 being responsible for the trimethylating activity. However, the preserved H3K4me2 bands in *atx2* leaf chromatin suggested that ATX2 was not involved in modifying *WRKY70* nucleosomes. *ACTIN*-specific bands amplified from the same *atx1* and *atx2* leaf chromatin templates provided evidence for the specificity of the *WRKY70* methylation patterns.

DISCUSSION

Divergence of *ATX1* and *ATX2* Promoter Functions

ATX1 and *ATX2* originated as a result of a segmental duplication involving the tip of chromosome 1 and an internal section of chromosome 2 (Baumbusch et al., 2001; Figure 1A). At least two rounds of duplications might have occurred in *Arabidopsis* resulting in mosaic rearrangements and segmental duplications. Most duplication blocks are estimated to have occurred 20 to 40

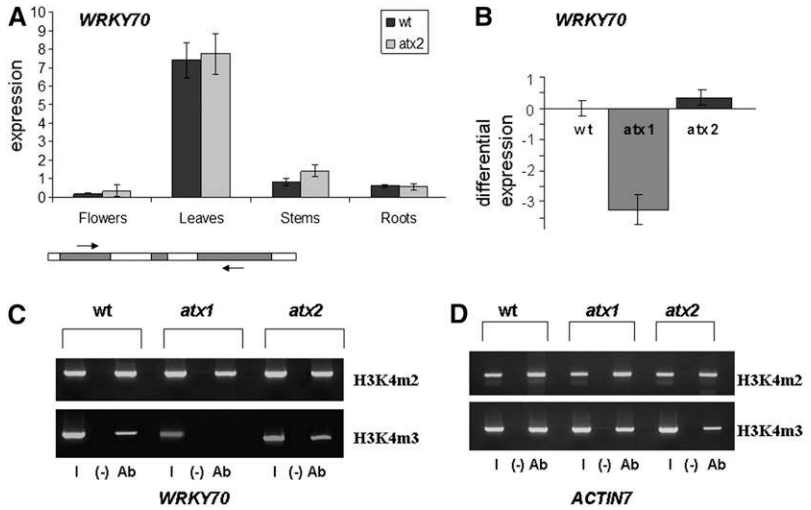

Figure 7. Expression and H3K4 Methylation Patterns of *WRKY70* in Wild-Type, *atx1*, and *atx2* Chromatin.

(A) Real-time PCR showing the tissue-specific expression of the *WRKY70* gene in wild-type and *atx2* backgrounds (mean ± SE, $n = 3$).
(B) Differential expression of *WRKY70* in *atx1* and *atx2* rosette leaves (mean ± SE, $n = 3$). The expression in the wild-type leaves is taken as level zero. Bars represent SD.
(C) *WRKY70* amplified from ChIP assays of wild-type, *atx1*, and *atx2* flower chromatin immunoprecipitated with antibodies distinguishing between di- and trimethylated H3K4 isoforms. Labeling is as in Figure 5C. A schematic illustration of the *WRKY70* gene including the regions amplified for the ChIP assay is shown at top of the panel.
(D) As in **(C)**, except that K4 methylation patterns of the housekeeping gene *ACTIN7* are shown as a control for the quality of the chromatins used as templates.

million years ago, before the evolution of the genus *Brassica* but after the separation of Brassicaceae from other close eudicot families (Simillion et al., 2002; Blanc et al., 2003).

The absence of visible *atx2*-related phenotypes, as well as the inability of ATX2 to substitute for ATX1 in an *atx1* background, could indicate that *ATX2* has become nonfunctional after the duplication, while the ancestral function has been retained by *ATX1*. However, it is important to emphasize that the phenotypes of *atx2* mutant plants have been scored under laboratory growth conditions, which cannot preclude a role for ATX2 in the survival and/or adaptation of the plant in the wild. Further cellular and molecular analyses confirmed the functional relevance of *ATX2*.

In agreement with models predicting that changes in *cis*-regulatory modules (promoters) of duplicated genes might lead to specific shifts in expression patterns between paralogs (Gu, 2003; He and Zhang, 2005; Duarte et al., 2006), we found more putative TF binding sites upstream of *ATX1* than of *ATX2* (see Supplemental Figure 2 online). All motifs from the *ATX2* promoter region are also present in the *ATX1* promoter region, indicating that similar regulation of the two genes is possible as well. In addition, unrecognized TF binding sites and/or specific combinations of known motifs in the *ATX2* promoter may guide its specific expression as seen, for instance, in 2-week-old roots and in pollen (Figures 3B and 3D). Although it appears that the *ATX2* promoter may have lost upstream regulatory sequences, we do not exclude the acquisition of novel unrecognized motifs or changes in the modular combinations of TF binding boxes. These could lead to expression pattern shifts between the paralogs and allow the divergence of their functions (Wendel, 2000; Hughes, 2002; Duarte et al., 2006).

Nonredundant Roles of ATX1 and ATX2 in Overall Gene Regulation

The lower number of misexpressed genes in *atx2* mutants compared with *atx1* (Alvarez-Venegas et al., 2006a) is in accordance with a more restricted role for ATX2 in *Arabidopsis.* Approximately 40% of ATX2-regulated genes overlap with ATX1-regulated genes. These results, together with the largely nonoverlapping patterns of *ATX1* and *ATX2* expression, suggest nonredundant functions. Within the shared targets, only eight genes were similarly influenced in the *atx1* and *atx2* backgrounds compatible with redundant functions. The expression of most of the overlapping genes was oppositely influenced in the *atx1* and *atx2* backgrounds, suggesting that ATX1 and ATX2 might participate in specific antagonistic complexes. Another possibility is that ATX1 and ATX2 regulate different TFs with opposite effects on the expression of shared targets.

To explore the mechanisms behind the apparently redundant or antagonistic effects at the molecular level, we examined the HKMT activity of ATX2. Recombinant Trithorax-related proteins of yeast, animal, or plant origin do not display robust methyltransferase activity (Czermin et al., 2002; Milne et al., 2002; Alvarez-Venegas et al., 2003), making it impractical to analyze enzyme activity by in vitro biochemical approaches. The lack of detectable ATX2 involvement in overall H3K4 methylation could indicate that ATX2 has no enzyme activity, that redundant enzymes compensate for ATX2 loss, or that ATX2 modifies only a limited nucleosomal fraction. Analyses of selected shared loci allowed us to reveal ATX2 enzyme activity and the divergence of ATX1 and ATX2 biochemical functions.

Different Roles and Molecular Mechanisms Used by ATX1 and ATX2 to Regulate Shared Targets

ATX1 and ATX2 upregulate the transcription of the *NAP* gene. Reciprocal changes of its nucleosomal patterns in *atx1* and *atx2* mutant chromatins suggested a molecular basis for this synergy. The lack of H3K4me2 signals on *atx2 NAP* nucleosomes defines ATX2 as a putative H3K4 dimethyltransferase involved in their dimethylation (Figure 5C). Furthermore, although both ATX1 and ATX2 upregulate the *XTH33* gene, they use different mechanisms. While ATX2 is implicated in the deposition of the H3K4me2 marks, ATX1 does not modify the *XTH33* nucleosomes, suggesting that its effect is indirect (Figure 6B). Moreover, trimethylation of H3K4 is not a requirement for *XTH33* transcription (Figures 6A and 6C).

ATX1 and ATX2 are differentially involved in the regulation of *WRKY70* as well. In leaves, ATX2 does not influence *WRKY70* transcription and does not participate in generating the *WRKY70*- H3K4me2 marks. The presence of H3K4me2 tags on *WRKY70* nucleosomes from *atx2* chromatin suggests that a different dimethyltransferase is involved. By contrast, ATX1 modifies *WRKY70* nucleosomes and stimulates *WRKY70* transcription (Figures 7B and 7C).

Collectively, the results demonstrate that ATX1 and ATX2 have evolved different target specificity and use different molecular and biochemical mechanisms when regulating shared targets. However, they do not allow us to exclude a potential ability of ATX2 to carry out trimethylation or of ATX1 to dimethylate nucleosomal K4 at other gene loci.

It is unclear what determines the di- and trimethylating activities of ATX2 and ATX1, respectively. The aromatic ring amino acid at position 4 in the conserved motif ELx(F/Y/W/)DY is important for the specificity of the SET domain peptide in establishing mono-, di-, or trimethylation of a single Lys residue (Zhang et al., 2003; Cheng et al., 2005; Collins, et al., 2005; Thorstensen et al., 2006). Generally, proteins carrying W or F are involved in H3K9me3, while those carrying Y act as mono- and dimethyltransferases (Jackson et al., 2002, 2004; Cheng et al., 2005; Collins et al., 2005; Ebbs and Bender, 2006; Casas-Mollano et al., 2007). Interestingly, F/Y substitution may alter the substrate specificity, underscoring the significance of this amino acid in defining tri- versus dimethyltransferase activity (Cheng et al., 2005; Collins et al., 2005). It is important to emphasize, however, that this correlation has been demonstrated only for SET peptides of the SUVAR family. By contrast, all members of the trithorax SET domain family have an invariant Y and still they can perform trimethylations (this report; Santos-Rosa et al., 2002; Wysocka et al., 2005; Ruthenberg et al., 2007). Therefore, the presence of a Y in the active site of Trithorax-type SET peptides, apparently, is not restrictive to the trimethylation of K4. Furthermore, recombinant SUVAR SET domain peptides display robust HKMTase activity, while the trithorax SET domains require partners to be able to methylate H3K4 in vitro (Petruk et al., 2001; Milne et al., 2002; Nakamura et al., 2002). It seems that the steric requirements for the deposition of the substrate and the conformation of the product at the active site of the Trithorax SET domain are different from those governing the SUVAR SET domain.

In contrast with the actively studied roles of histone K4 di and trimethylations as chromatin marks, the significance of monomethylated H3K4 has remained elusive. In *Chlamydomonas*, a separate activity is involved in generating K4me1, which tends to act as a silencing chromatin mark (van Dijk et al., 2005). However, animal- or plant-specific K4 monomethyltransferases have not been identified so far, despite the abundance of H3K4me1 marks in *Arabidopsis* chromatin (Zhang et al., 2007). It remains to be established whether K4me1 marks are labeling nucleosomes associated with coding sequences and whether they are reflective of gene transcription states. Preliminary results suggest that ATX1 and ATX2 are not responsible for genome-wide K4me1 modification. Whether they are involved in monomethylation could not be determined reliably due to the low K4me1 levels at the loci studied here. We shall need better tools than those currently available to provide conclusive answers to this question. Isolation and characterization of specific complexes assembled by ATX1 or ATX2, as well as structural analysis of the ATX SET domain peptides, will be critical steps toward overcoming the obstacles for direct biochemical assessment of Trithorax function.

METHODS

Plant Material and Growth Conditions

Arabidopsis thaliana Col-0 seeds were sterilized and grown either in 40 mL of germination media or in pots at 24°C under long-day (16 h light/8 h darkness) or short-day (9 h light/15 h darkness) light cycles, as indicated. Seeds were pretreated by exposure to cold (4°C) for 48 h, and all experimental and control lines were handled under the same conditions. Three *Ti*-insertion lines (SALK_074806, SALK_117262, and SALK_001880) obtained from the *Arabidopsis* stock center were analyzed after kanamycin selection of seeds grown in agar plates and media (2.25 g Murashige and Skoog salts [Sigma-Aldrich] and 10 g sucrose per liter, pH 6.0) containing 50 μg/mL kanamycin. Kanamycin-resistant plants were screened for homzygosity by PCR genotyping.

PCR Genotyping

All PCRs were done in 25 μL: 5 min at 95°C, followed by 35 cycles of 95°C for 30 s, 56°C for 30 s, 72°C for 2 min, and a final cycle of 72°C for 5 min. Primers used for genotyping were those suggested by the Salk Institute Genomic Analysis Laboratory ''iSec Tools'' (http://signal.salk.edu/tdnaprimers.2.html) and generated with the default conditions.

Template Preparation

All DNA extractions were performed with DNAzol reagent (Invitrogen) following the manufacturer's instructions.

The first line did not produce the expected PCR-generated profiles and was discarded; homozygous mutant lines, identified and propagated by selfing from lines SALK_001880 and SALK_117262, were named *atx2-1* and *atx2-2*, respectively. The *atx1* mutant line was described by Alvarez-Venegas et al. (2003).

Promoter Analysis

For cloning the promoter regions, we included the sequences lying between the transcription start sites of *ATX1* or *ATX2* and the end of the respective upstream neighbor gene. The designed promoters included the 5′ untranslated regions of *ATX1* or *ATX2*. Primers begin with a six-nonsense nucleotide sequence, followed by the restriction sequence (in capital letters below) used in the cloning step, followed then by the

respective genomic sequence. Primers for the *ATX1* and *ATX2* promoters used in this study were as follows: (*ATX1*) forward, 5′-cgatgcGGATCCtctccgtggagtttgagaatcc-3′, reverse, 5′-tcagacCCATGGggagattattcggagggagaaagc-3′; (*ATX2*) forward, 5′-ctaagcGGATCCgtgcatacacatgtag-3′, reverse, 5′-atccatGGCCATtcaaaggaggagagtaag-3′.

DNA sequences amplified from DNA template under PCR conditions as those described for the PCR genotyping were cloned in the pCambia1303 vector (Canberra), replacing the original 35S promoter with the desired experimental sequence. Constructs were verified by sequencing, and the plasmids were introduced in *Arabidopsis* plants by the dip infiltration method (Clough and Bent, 1998) to produce transgenic GUS-expressing lines. Six independently transformed lines were selected for each transformed construct and analyzed for GUS expression. Staining was done according to Silverstone et al. (1997). Color appeared after 4 h but was allowed to develop overnight. Samples were examined under a Nikon SMZ800 dissecting microscope equipped with an Optronics digital camera and MagnaFire 2.1 software. Single-copy insertion lines were used in the comparative experiments. For analyses of TF binding motifs, information available from the Ohio State University site was used (http://arabidopsis.med.ohio-state.edu/AtcisDB).

RNA Sample and Microarray Preparation

atx1, *atx2-2*, and wild-type control plants were grown and handled under identical conditions. Tissues were collected from whole, 4-week-old plants. For each experiment and its separate control, total RNA was isolated from two plants and frozen in liquid nitrogen using the TRIzol reagent following the manufacturer's instructions (Invitrogen) and further purified using a Qiagen RNeasy column. Fifteen micrograms of total RNA was used to synthesize cDNA using the Affymetrix One-Cycle cDNA synthesis kit according to the manufacturer's instructions. All sample preparations followed the protocols of the Affymetrix GeneChip Expression Analysis Technical manual. Hybridizations were performed on Affymetrix *Arabidopsis* Genome ATH1-121501 arrays, stained with streptavidin-phycoerythrin conjugate on an Affymetrix Fluidics Station 450. Images were obtained using the GeneChip 3000. More data and discussion of hybridization experiments in the *atx1* background are available elsewhere (Alvarez-Venegas et al., 2006a).

Microarray Data Analysis

We used Affymetrix ATH1-121501 microarrays that cover 23,489 genes using 22,810 probe sets. Probes were mapped to genes using the 2006 Arabidopsis Information Resource gene annotation (ftp://ftp.arabidopsis.org/home/tair/Microarrays/Affymetrix/) that represents a major improvement over the original 2001 annotation in the Affymetrix GCOS software. Since correcting by the mismatched probes now is believed to increase the noise (Irizarry et al., 2006), we used only the perfectly matched probes. The quality of hybridization was assessed by MvA plots, pairwise correlation, and RNA degradation. Statistical analyses were performed using the *Bioconductor* suite (Gentleman et al., 2004) implemented in the *R* programming language (Dalgaard, 2002). Raw intensity measurements were background corrected and quantile normalized (Irizarry et al., 2003a) using robust multiarray average analysis (Irizarry et al., 2003b) implemented in the *affy* package (Gautier et al., 2004). The background-corrected, normalized, and $\log_2$-transformed expression values were fitted to a linear model using the *limma* package (Smyth, 2004). Linear models were refined by an empirical Bayes method. The resulting P values were subjected to multiple test corrections. Since the number of downregulated genes exceeded the number of upregulated transcripts, a condition that may have biased the false discovery rate (Benjamini and Hochberg, 1995) calculations, multiple test corrections were performed by the more robust and conservative Bonferroni method.

Overall Histone H3-K4 Methylation in the Wild Type and *atx2* and *atx1* Mutants

Total histones extracted from 3-week-old wild-type and *atx1* mutant plants were probed with antibodies specific for di- or trimethylated H3K4in protein gel blots exactly as described earlier (Alvarez-Venegas and Avramova, 2005). Membranes then were stripped and reprobed with antibodies specific for nonmodified histone H3. The levels of histone H3-tail methylation of wild-type histones, defined as the ratio of mK/H3-to-H3 intensity signals, were computed from four independent experiments.

RT-PCR

RT-PCR analysis was done exactly as described in Saleh et al. (2007) using the following primers: *NAP*, forward, 5′-tcctaccgacgaagaactcatcgt-3′, reverse, 5′-taaacatcgcttgacgatgatggt-3′; *ATX2* (band a; see Supplemental Figure 1 online), forward, 5′-GACTCGCCCTGTTTTCAGAG-3′, reverse, 5′-GCCTCTAGCAAAATGAAAGC-3′; *ATX2* (band b; see Supplemental Figure 1 online), forward, 5′-GGAACCTGAAGCTCTTGCTG-3′, reverse, 5′-GCATCTTGCGAAACCACAGT-3′;

Real-Time PCR Analysis

Total RNA was isolated using the Invisorb Spin Plant RNA Mini kit (Invitek) according to the manufacturer's instructions. First-strand cDNA synthesis was performed on 500 ng of RNA using the M-MLV System for RT-PCR (Invitrogen). Real-time PCR reactions were performed in a final volume of 25 μL containing 12.5 μL of iQ SYBR Green PCR supermix (Bio-Rad), 1 μL of each primer (forward and reverse, 50 ng/μL), 5 μL of cDNA (1 ng/μL), and 6.5 μL sterile deionized water. The PCR products were amplified under the following conditions: 95°C for 3 min, 39 cycles of 95°C for 30 s, 52°C for 30 s, and 72°C for 10 min using an iCycler iQ real-time PCR detection system (Bio-Rad), iQ 96-well PCR plates (Bio-Rad), and optical quality sealing tapes (Bio-Rad). The *ACTIN7* gene sequence was used as an internal control. The primer sequences were as follows: *NAP*, forward, 5′-tcatggacgaagtactaatggagg-3′, reverse, 5′-tagactccgaatcaggttgatgaag-3′; *XTH33*, forward, 5′-TTGGTTTCTTCACACAGCAGGAA-3′, reverse, 5′-GCACTCAGCAGGCATGACTTT-3′; *WRKY70*, forward, 5′-CAAGAGCAAGACTTGTGACCATCAT-3′, reverse, 5′-AATCTTCTTCGAAAACCATTTCTGG-3′, *ACTIN7*, forward, 5′-CTACGAGGGGTATGCTCTTCCTCAT-3′, reverse, 5′-CTGAAGAACTGCTCTTGGCTGTCTC-3′.

ChIP Assays

A protocol described earlier (Alvarez-Venegas and Avramova, 2005) was used with some modifications: harvested tissues from examined plant samples were cross-linked (0.4 M sucrose, 10 mM Tris, pH 8, 1 mM EDTA, 1 mM PMSF, and 1% formaldehyde) under vacuum, followed by freezing and grinding in liquid nitrogen. After resuspension in buffer (15 mM PIPES, pH 6.8, 5 mM $MgCl_2$, 60 mM KCl, 0.25 M sucrose, 15 mM NaCl, 1 mM $CaCl_2$, 0.9% Triton X-100, 1 mM PMSF, 2 μg/mL pepstatin A, and 2 μg/mL aprotinin), the slurry was filtered (four layers of cheesecloth) and the filtrate centrifuged at 10,000*g* for 20 min in a Sorvall SA-600 rotor. The nuclear pellet, resuspended in lysis buffer (50 mM HEPES, pH 7.5, 150 mM NaCl, 1 mM EDTA, 1% Triton X-100, 0.1% deoxycholate, 0.1% SDS, 1 mM PMSF, 1 μg/mL aprotinin, 1 μg/mL pepstatin A), was sonicated to shear the DNA. After removing cell debris (centrifugation at 13,000 rpm in cold benchtop centrifuge for 10 min), the chromatin fraction was harvested and used for immunoprecipitation. Antitrimethyl Histone H3 Lysine4 (K4) (Upstate) and antidimethyl Histone H3K4 (Upstate) were used. Negative control samples were treated in the same way, except without antibodies added. Each immunoprecipitation was performed in at least three separate experiments. Calibration curves were built to determine optimal amounts of chromatin to be used in each experiment and to

ensure equivalent amounts of starting material (Alvarez-Venegas and Avramova, 2005). The PCR products were amplified under the following conditions: 95°C for 3 min, 38 cycles of 94°C for 30 s, 50°C for 30 s, 72°C for 1 min, and 72°C for 10 min. The primer sequences used were as follows: *WRKY70*, forward, 5′-AGCAACTCCTCTCTCAACCCG-3′, reverse, 5′-CCATTGACGTAACTGGCCTGA-3′; *XTH33*, forward, 5′-TTGGTTTC-TTCACACAGCAGGAA-3′, reverse, 5′-GCACTCAGCAGGCATGACTTT-3′; *NAP*, forward, 5′-tccctccagggttcagatttc-3′, reverse, 5′-catcgcttgacg-atgatggtt-3′; *ACTIN7*, forward, 5′-ggtgaggatattcagccacttgtctg-3′, reverse, 5′-tgtgagatcccgacccgcaagatc-3′.

Accession Numbers

Sequence data from this article can be found in the Arabidopsis Genome Initiative or GenBank/EMBL databases under the following accession numbers: At2g31650 (*ATX1*), At1g05830 (*ATX2*), At5g09810 (*ACTIN7*), At1g69490 (*NAP*), At3g56400 (*WRKY70*), and At1g10550 (*XTH33*).

Supplemental Data

The following materials are available in the online version of this article.

Supplemental Figure 1. Expression of *ATX2* in Different Genetic Backgrounds and Delayed Abscission Phenotypes in *atx1* and *atx2* Flowers.

Supplemental Figure 2. Transcription Factor Binding Motifs Recognized in the Promoter Regions of *ATX1* and *ATX2*.

Supplemental Figure 3. Overall Histone H3-K4 Methylation in Wild-Type and in *atx2-2* Plants.

Supplemental Figure 4. Real-time PCR Tissue-Specific Expression Analysis of *XTH33*.

Supplemental Table 1. *atx2* Flowers Defective in Flower Organ Abscission.

Supplemental Data Set 1. Upregulated Genes in the *atx2* Background.

Supplemental Data Set 2. Downregulated Genes in the *atx2* Background.

ACKNOWLEDGMENTS

This article is dedicated to the memory of Roumen Tsanev, a pioneer in chromatin research and an inspiring teacher in epigenetics. This study was partially supported by the NSF-MCB-0343934 grant award to Z.A.

Received October 31, 2007; revised February 21, 2008; accepted March 11, 2008; published March 28, 2008.

REFERENCES

Alvarez-Venegas, R., Al Abdallat, A., Guo, M., Alfano, J.P., and Avramova, Z. (2007a). Epigenetic control of a transcription factor at the cross section of two antagonistic pathways. Epigenetics **2:** 106–113.

Alvarez-Venegas, R., and Avramova, Z. (2001). Two *Arabidopsis* homologs of the animal *trithorax* genes; A new structural domain is a signature feature of the trithorax family. Gene **271:** 215–221.

Alvarez-Venegas, R., and Avramova, Z. (2002). The SET-domain proteins of the Su(var)3-9, E(z), and Trithorax families. Gene **285:** 25–37.

Alvarez-Venegas, R., and Avramova, Z. (2005). Methylation patterns of histone H3 Lys 4, Lys 9 and Lys 27 in transcriptionally active and inactive *Arabidopsis* genes and in *atx1* mutants. Nucleic Acids Res. **33:** 5199–5207.

Alvarez-Venegas, R., Pien, S., Sadder, M., Witmer, X., Grossnicklaus, U., and Avramova, Z. (2003). *ATX1*, an *Arabidopsis* homolog of *Trithorax* has histone methylase activity and activates flower homeotic genes. Curr. Biol. **13:** 627–634.

Alvarez-Venegas, R., Sadder, M., Hlavacka, A., Baluška, F., Xia, Y., Lu, G., Firsov, A., Sarath, G., Moriyama, H., Dubrovsky, J., and Avramova, Z. (2006a). The Arabidopsis homolog of trithorax, ATX1, binds phosphoinositide 5-phosphate and the two regulate a common set of target genes. Proc. Natl. Acad. Sci. USA **103:** 6049–6054.

Alvarez-Venegas, R., Sadder, M., Tikhonov, A., and Avramova, Z. (2007b). Origin of the bacterial *SET* domain genes: Vertical or horizontal? Mol. Biol. Evol. **24:** 482–497.

Alvarez-Venegas, R., Xia, Y., Lu, G., and Avramova, Z. (2006b). Phosphoinositide 5-phosphate and phosphoinositide 4-phosphate trigger distinct specific responses of *Arabidopsis* genes. Plant Signal Behav. **1:** 140–149.

Baumbusch, L.O., Thorstensen, T., Krauss, V., Fischer, A., Naumann, K., Assalkhou, R., Schiltz, I., Reuter, G., and Aalen, R.B. (2001). The *Arabidopsis thaliana* genome contains at least 29 active genes encoding SET-domain proteins that can be assigned to four evolutionary conserved classes. Nucleic Acids Res. **29:** 4319–4327.

Becnel, J., Natarajan, M., Kipp, A., and Braam, J. (2006). Developmental expression patterns of Arabidopsis XTH genes reported by transgenes and Genevestigator. Plant Mol. Biol. **61:** 451–467.

Benjamini, Y., and Hochberg, Y. (1995). Controlling the false discovery rate: A practical and powerful approach to multiple hypothesis testing. J. R. Stat. Soc. B **57:** 289–300.

Bernstein, B.E., Humphrey, E.L., Erlich, R.L., Schneider, R., Bouman, P., Liu, J.S., Kouzarides, T., and Schreiber, S.L. (2002). Methylation of histone H3 Lys 4 in coding regions of active genes. Proc. Natl. Acad. Sci. USA **99:** 8695–8700.

Blanc, G., Hokamp, K., and Wolfe, K.H. (2003). A recent polyploidy superimposed on older large-scale duplications in the *Arabidopsis* genome. Genome Res. **13:** 137–144.

Blanc, G., and Wolfe, K.H. (2004). Functional divergence of duplicated genes formed by polyploidy during Arabidopsis evolution. Plant Cell **16:** 1679–1691.

Casas-Mollano, J.A., van Dijk, K., Eisenhart, J., and Cerutti, H. (2007). SET3p monomethylates histone H3 on lysine 9 and is required for the silencing of tandemly repeated transgenes in Chlamydomonas. Nucleic Acids Res. **35:** 939–950.

Cheng, X., Collins, R.E., and Zhang, X. (2005). Structural and sequence motifs of protein (histone) methylation enzymes. Annu. Rev. Biophys. Biomol. Struct. **34:** 267–294.

Clough, S.J., and Bent, A.F. (1998). Floral dip: A simplified method for Agrobacterium-mediated transformation of *Arabidopsis thaliana.* Plant J. **16:** 735–743.

Collins, R.E., Tachibana, M., Tamaru, H., Smith, K.M., Jia, D., Zhang, X., Selker, E.U., Shinkai, Y., and Cheng, X. (2005). *In vitro* and *in vivo* analyses of a Phe/Tyr switch controlling product specificity of histone lysine methyltransferases. J. Biol. Chem. **280:** 5563–5570.

Czermin, B., Melfi, R., McCabe, D., Setz, V., Imhof, A., and Pirrotta, V. (2002). Drosophila enhancer of zeste/ESC complexes have a histone H3 methyltransferase activity that marks the chromosomal polycomb sites. Cell **111:** 185–196.

Dalgaard, P. (2002). Introductory Statistics with R. (Berlin: Springer).

Divol, F., Vilaine, F., Thibivilliers, S., Kusiak, C., Sauge, M.H., and Dinant, S. (2007). Involvement of the xyloglucan endotransglycosylase/hydrolases encoded by celery XTH1 and *Arabidopsis* XTH33 in the phloem response to aphids. Plant Cell Environ. **30:** 187–201.

Duarte, J.M., Cui, L., Wall, P.K., Zhang, Q., Zhang, X., Leebens-Mack, J., Ma, H., Altman, N., and dePamphilis, C.W. (2006).

Expression pattern shift following duplication indicative of subfractionalization and neofractionalization in regulatory genes in Arabidopsis. Mol. Biol. Evol. **23:** 469–478.

Ebbs, M.L., and Bender, J. (2006). Locus-specific control of DNA methylation by the *Arabidopsis* SUVH5 histone methyltransferase. Plant Cell **18:** 1166–1176.

Gautier, L., Cope, L., Bolstad, B.M., and Irizarry, R.A. (2004). Analysis of Affymetrix GeneChip data at the probe level. Bioinformatics **20:** 307–315.

Gentleman, R.C., et al. (2004). Bioconductor: Open software development for computational biology and bioinformatics. Genome Biol. **5:** R80.

Gu, X. (2003). Evolution of duplicate genes versus genetic robustness against null mutations. Trends Genet. **19:** 354–356.

Hayashi, K., Yoshida, K., and Matsui, Y. (2005). A histone H3 methyltransferase controls epigenetic events required for meiotic prophase. Nature **438:** 374–378.

He, X., and Zhang, J. (2005). Gene complexity and gene duplicability. Curr. Biol. **15:** 1016–1021.

Hughes, A.L. (2002). Adaptive evolution after gene duplication. Trends Genet. **18:** 433–434.

Irizarry, R.A., Bolstad, B.M., Collin, F., Cope, L.M., Hobbs, B., and Speed, T.P. (2003a). Summaries of Affymetrix GeneChip probe level data. Nucleic Acids Res. **31:** e15.

Irizarry, R.A., Hobbs, B., Collin, F., Beazer-Barclay, Y.D., Antonellis, K.J., Scherf, U., and Speed, T.P. (2003b). Exploration, normalization, and summaries of high density oligonucleotide array probe level data. Biostatistics **4:** 249–264.

Irizarry, R.A., Wu, Z., and Jaffee, H.A. (2006). Comparison of Affymetrix GeneChip expression measures. Bioinformatics **22:** 789–794.

Jackson, J.P., Lindroth, A.M., Cao, X., and Jacobsen, S.E. (2002). Control of CpNpG DNA methylation by the KRYPTONITE histone H3 methyltransferase. Nature **416:** 556–560.

Jasencakova, Z., Soppe, W.J.J., Meister, A., Gernand, D., Turner, B.M., and Schubert, I. (2003). Histone modifications in Arabidopsis-high methylation of H3 lysine9 is dispensable for constitutive heterochromatin. Plant J. **33:** 471–480.

Kim, S.Y., He, Y., Jacob, Y., Noh, Y.S., Michaels, S., and Amasino, R. (2005). Establishment of the vernalization-responsive, winter-annual habit in *Arabidopsis* requires a putative histone H3 methyl transferase. Plant Cell **17:** 3301–3310.

Kondrashov, F.A., Rogozin, I.B., Wolf, Y.I., and Koonin, E.V. (2002). Selection in the evolution of gene duplication. Genome Biol. **2:** 8.1–8.9.

Kouzarides, T. (2007). Chromatin modifications and their function. Cell **128:** 693–705.

Krauss, V., Fassl, A., Fiebig, P., Patties, I., and Sass, H. (2006). The evolution of the histone methyltransferase gene Su(var)3-9 in metazoans includes a fusion and re-fusion from a functionally unrelated gene. BMC Evol. Biol. **6:** 1–15.

Li, J., Brader, G., Kariola, T., and Palva, E.T. (2006). WRKY70 modulates the selection of signaling pathways in plant defense. Plant J. **46:** 477–491.

Li, J., Brader, G., and Palva, E.T. (2004). The WRKY70 transcription factor: A node of convergence for jasmonate-mediated and salicylate-mediated signals in plant defense. Plant Cell **16:** 319–331.

Lippman, Z., et al. (2004). Role of transposable elements in heterochromatin and epigenetic control. Nature **430:** 471–476.

Milne, T.A., Briggs, S.D., Brock, H.W., Martin, M.E., Gibbs, D., Allis, C.D., and Hess, J.L. (2002). MLL targets SET domain methyltransferase activity to Hox gene promoters. Mol. Cell **10:** 1107–1117.

Nakamura, T., Mori, T., Tada, S., Krajewski, W., Rozovskaya, T., Wassell, R., Dubois, G., Mazo, A., Croce, C., and Canaani, E. (2002). ALL-1 is a histone methyltransferase that assembles a supercomplex of proteins involved in transcriptional regulation. Mol. Cell **10:** 1119–1128.

Ng, H., Robert, F., Young, R., and Struhl, K. (2003). Targeted recruitment of SET1 histone methyltransferase by elongating Pol II provides a localized mark and memory of recent transcriptional activity. Mol. Cell **11:** 709–719.

Ohno, S. (1970). Evolution by Gene Duplication. (New York: Springer).

Petruk, S., Sedkov, Y., Smith, S., Tilib, S., Kraevski, V., Nakamura, T., Canaani, E., Croce, C.M., and Mazo, A. (2001). trithorax and dCBP acting in complex to maintain expression of a homeotic gene. Science **294:** 1331–1334.

Pickett, F.B., and Meeks-Wagner, D.R. (1995). Seeing double: Appreciating genetic redundancy. Plant Cell **7:** 1347–1356.

Rea, S., Eisenhaber, F., O'Carroll, D., Strahl, B.D., Sun, Z.W., Schmidt, M., Opravil, S., Mechtler, K., Pontig, C.P., Allis, C.D., and Jenuwein, T. (2000). Regulation of chromatin structure by site-specific histone H3 methyltransferases. Nature **406:** 593–599.

Ruthenberg, A.J., Allis, C.D., and Wysocka, J. (2007). Methylation of lysine 4 on histone h3: Intricacy of writing and reading a single epigenetic mark. Mol. Cell **25:** 15–30.

Sablowski, R.W., and Meyerowitz, E. (1998). A homolog of NO APICAL MERISTEM is an immediate target of the floral homeotic genes APETALA3/PISTILLATA. Cell **92:** 93–103.

Saleh, A., Al-Abdallat, A., Ndamukong, I., Alvarez-Venegas, R., and Avramova, Z. (2007). The *Arabidopsis* homologs of trithorax (ATX1) and enhancer of zeste (CLF) establish ''bivalent chromatin marks'' at the silent *AGAMOUS* locus. Nucleic Acids Res. **35:** 6290–6296.

Santos-Rosa, H., Schneider, R., Bannister, A.J., Sherriff, J., Bernstein, B.E., Emre, T., Schreiber, S.L., Mellor, J., and Kouzarides, T. (2002). Active genes are tri-methylated at K4 of histone H3. Nature **419:** 407–411.

Silverstone, A.L., Chang, C., Krol, E., and Sun, T.P. (1997). Developmental regulation of the gibberellin biosynthetic gene GA1 in *Arabidopsis thaliana*. Plant J. **12:** 9–12.

Simillion, C., Vandepoele, K., Van, Montagu, M.C., Zabeau, M., and Van de Peer, Y. (2002). The hidden duplication past of *Arabidopsis thaliana.* Proc. Natl. Acad. Sci. USA **99:** 13627–13632.

Smyth, G.K. (2004). Linear models and empirical bayes methods for assessing differential expression in microarray experiments. Stat. Appl. Genet. Mol. Biol. **3:** Article 3.

Thorstensen, T., Fischer, A., Sandvik, S.V., Johnsen, S.S., Grini, P.E., Peuter, G., and Aalen, R.B. (2006). The Arabidopsis SUVR4 protein is a nucleolar histone methyltransferase with preference for monomethylated H3K9. Nucleic Acids Res. **34:** 5461–5470.

van Dijk, K., Marley, K.E., Jeong, B.R., Xu, J., Hesson, J., Cerny, R.L., Waterborg, J.H., and Cerutti, H. (2005). Monomethyl histone H3 lysine 4 as an epigenetic mark for silenced euchromatin in Chlamydomonas. Plant Cell **17:** 2439–2453.

Wendel, J. (2000). Genome evolution in polyploids. Plant Mol. Biol. **42:** 225–249.

Wysocka, J., Swigut, T., Milne, T., Dou, Y., Zhang, X., Burlingame, A., Roeder, R., Brivanlou, A., and Allis, D. (2005). WDR5 associates with histone H3 methylated at K4 and is essential for H3 K4 methylation and vertebrate development. Cell **121:** 859–872.

Zhang, K., Sridhar, V.V., Zhu, J., Kapoor, A., and Zhu, J.-K. (2007). Distinctive core histone post-translational modification patterns in Arabidopsis thaliana. PloS ONE. **2:** e1210.

Zhang, X., Yang, Z., Khan, S.I., Horton, J.R., Tamaru, H., Selker, E.U., and Cheng, X. (2003). Structural basis for the product specificity of histone lysine methyltransferases. Mol. Cell **12:** 177–185.

The Plant Cell, Vol. 28: 265, January 2016, www.plantcell.org

Correction

Saleh, A., Alvarez-Venegas, R., Yilmaz, M., Le, O., Hou, G., Sadder, M., Al-Abdallat, A., Xia, Y., Lu, G., Ladunga, I., and Avramova, Z. (2015). The highly similar *Arabidopsis* homologs of trithorax ATX1 and ATX2 encode proteins with divergent biochemical functions. Plant Cell **20:** 568–579.

Figure 7C (*WRKY70* ChIP-PCR assay) has been corrected to clarify that the wild-type control sample for H3K4m3 was run on a separate gel from the *atx1* and *atx2* samples, indicated by the space (white line, bottom row). The samples for H3K4m2 (top row) were run together on the same gel. The legend and labeling on the figure have been amended slightly for clarity. The original conclusions of the manuscript are unaltered by these corrections.

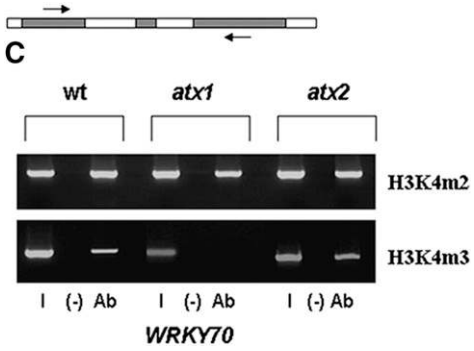

Figure 7. Original: Expression and H3K4 Methylation Patterns of *WRKY70* in Wild-Type, *atx1*, and *atx2* Chromatin.

(C) *WRKY70* amplified from ChIP assays of wild-type, *atx1*, and *atx2* flower chromatin immunoprecipitated with antibodies distinguishing between di- and trimethylated H3K4 isoforms. Labeling is as in Figure 5C. A schematic illustration of the *WRKY70* gene including the regions amplified for the ChIP assay is shown at top of the panel.

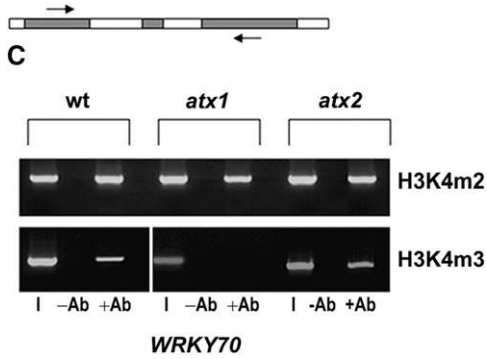

Figure 7. Corrected: Expression and H3K4 Methylation Patterns of *WRKY70* in Wild-Type, *atx1*, and *atx2* Chromatin.

(C) *WRKY70* amplified from ChIP assays of wild-type, *atx1*, and *atx2* flower chromatin immunoprecipitated with antibodies distinguishing between di- and trimethylated H3K4 isoforms. The control wild-type samples for H3K4m3, separated by a space (white line in the bottom panel), were resolved in a different gel from *atx1* and *atx2* samples. The blots were developed and processed in parallel. I, input sample representing 10% of the template amount used for the immunoprecipitation. −Ab and +Ab are immunoprecipitated chromatins without and with added antibody, respectively. A schematic illustration of the *WRKY70* gene including the regions amplified for the ChIP assay is shown at top of the panel.

Editor's note: the corrected figure and accompanying text were reviewed by members of *The Plant Cell* editorial board.

www.plantcell.org/cgi/doi/10.1105/tpc.15.01029

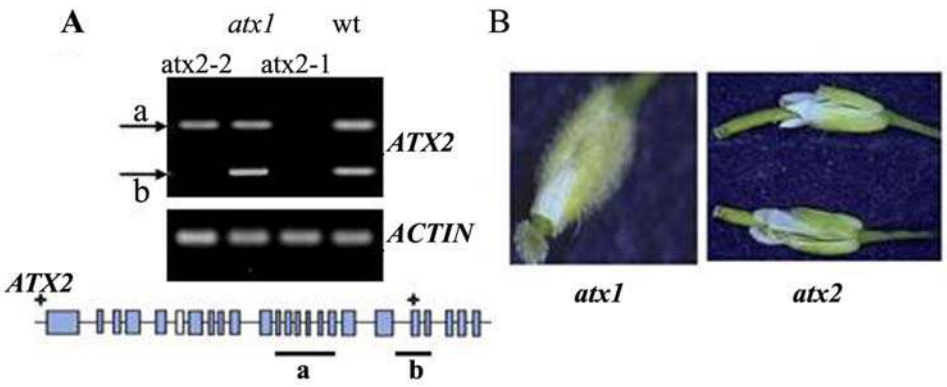

Supplemental Figure 1. Expression of *ATX2* in different genetic backgrounds and delayed abscission phenotypes in *atx1* and *atx2* flowers

A) *ATX2* expression in homozygous *Ti*-insertion lines by RT-PCR analysis. The regions amplified with specific primers are shown as bars below the *ATX2* gene map. The expected specific bands (**a** and **b**) recovered from the wt and in *atx1* templates serve as positive controls; neither band was recovered from the *atx2-1* sample, indicating that the *Ti*-insertion at the 5'-end of the gene abolished transcription of downstream sequences. (+) signs indicate the regions of *Ti*-insertions in the examined *atx2* backgrounds. In the *atx2-2* background, band (**b**) corresponding to sequences overlapping the area of the *Ti*-insertion (SET domain region) could not be recovered, while band (**a**) representing sequences located upstream of the *Ti*-insertion) was successfully amplified. Actin bands amplified from the respective templates were used as loading controls.
B) Aberrant abscission of flower organs after fertilization documented in about 20 % of flowers of the *atx1* and *atx2* backgrounds. Similar phenotypes were described in *nap* mutant, or *NAP*- overexpressing *Arabidopsis* plants (Sablowsky and Meyerowitz, 1998). These phenotypes were linked with *NAP*-misexpression (up-, or down-) disrupting the balance between cell division and cell expansion. It is possible that the phenotypes observed in *atx1* and *atx2* flowers are connected with lower *NAP*-levels.

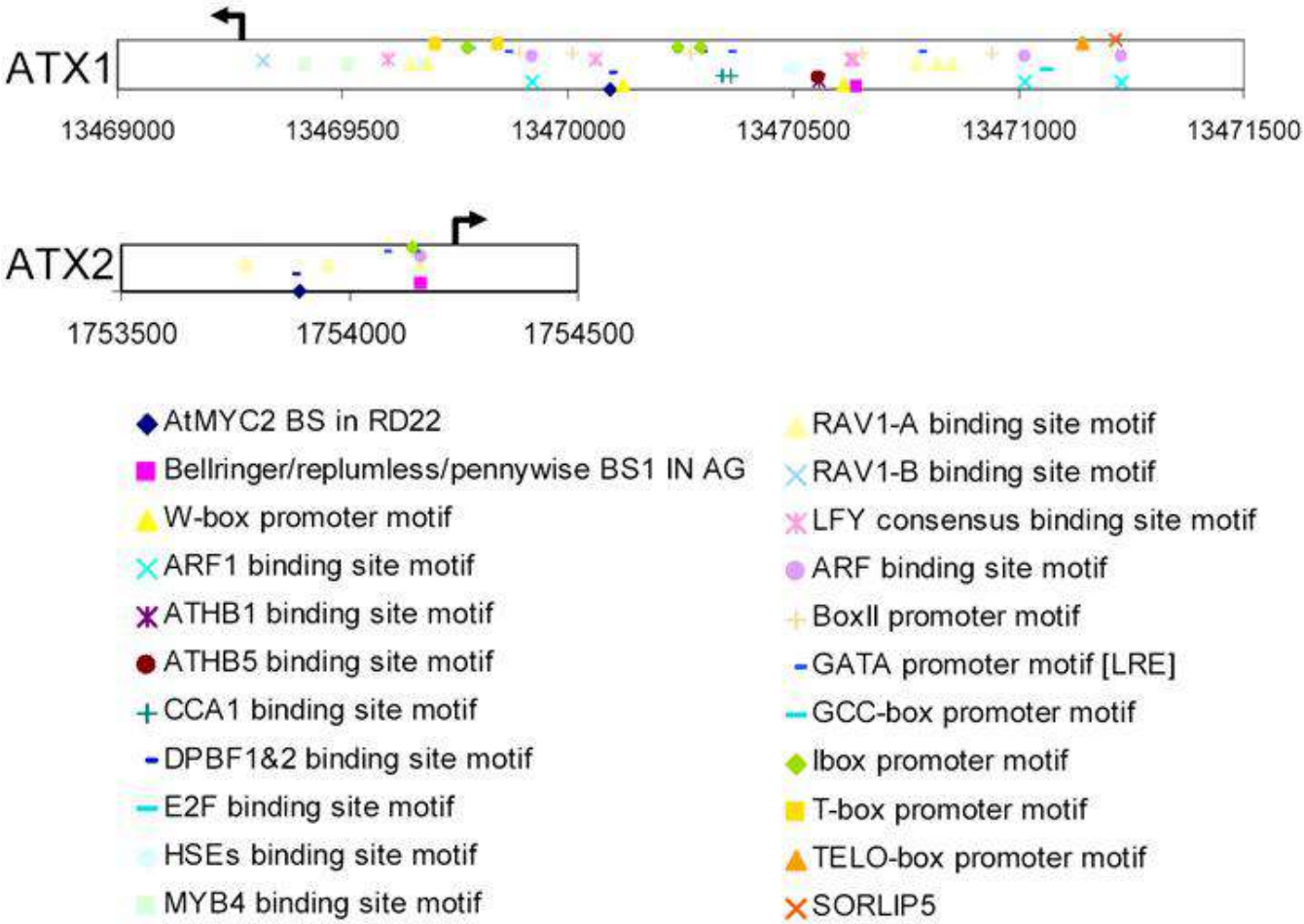

Supplemental Figure 2: Transcription factor binding motifs recognized in the promoter regions of *ATX1* and *ATX2*. Numbers indicate nucleotide coordinates on chromosomes 2 and 1, respectively.

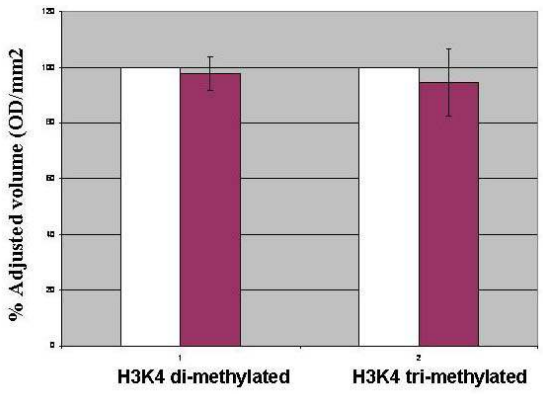

Supplemental Figure 3. Overall histone H3-K4 methylation in wild type and in *atx2-2* plants

Total histones extracted from 3-week old wild type and *atx2-2* mutant plants were probed with antibodies specific for di-, or tri-methylated K4/H3 in Western blots. Membranes were then stripped and re-probed with antibodies specific for non-modified histone H3. The levels of histone H3-tail methylation of wild type histones, defined as the ratio of mK/H3-to-H3 intensity signals, were taken as 100%. Quantization of band intensities and volume adjustments were done as described (Alvarez-Venegas and Avramova, 2005). Bars indicate standard deviation.

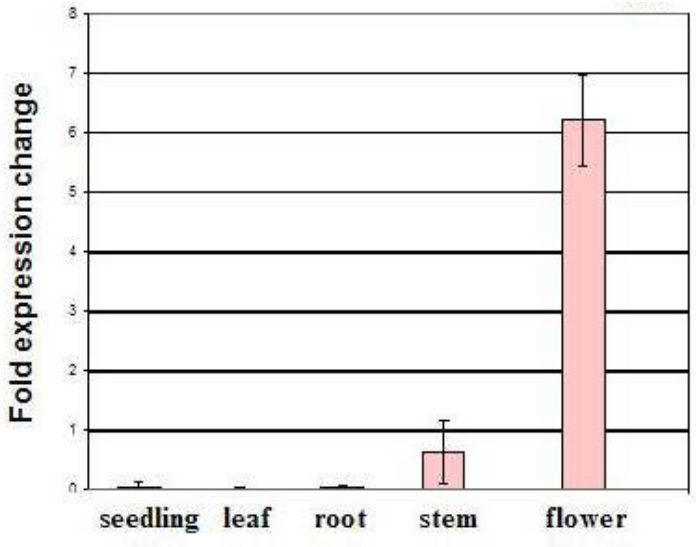

Supplemental Figure 4. Real-time PCR tissue-specific expression analysis of *XTH33* (n=3). Standard deviations are shown by bars.

Supplemental Table 1. *atx2* flowers defective in flower organ abscission

PLANT NUMBER	NUMBER OF FLOWERS	NUMBER OF DEFECTIVE FLOWERS	DEFECTIVE FLOWERS PER PLANT (%)
1	18	4	22.22
2	8	2	25.00
3	17	3	17.64
4	13	4	30.76
5	15	4	26.66
6	13	3	23.07
7	10	2	20.00
8	14	3	21.42
9	13	4	30.76
10	17	3	17.64
11	9	2	22.22
12	18	4	22.22
13	11	1	9.09
14	17	4	23.52
15	19	5	26.31
16	7	2	28.57
17	15	2	13.33
18	18	4	22.22
19	15	2	13.33
20	13	5	38.46
21	12	2	16.66
22	9	2	22.22
23	16	3	18.75
24	10	3	30.00
25	15	2	13.33
26	17	4	23.52
27	12	3	25.00
28	14	2	14.28
29	8	1	12.50
30	16	4	25.00
31	7	1	14.28
32	12	4	33.33
33	9	2	22.22
	Total	Total	Mean ± standard error
	460	96	21.98 ± 6.55